PCCP

Accepted Manuscript

ROYAL SOCIETY OF CHEMISTRY

www.rsc.org/pccp

Enhanced Stability of Zn_2SnO_4 with N719, N3 and EosinY Dye Molecules for DSSC Application

Partha Pratim Das [†£], Anurag Roy [†£] Sumita Das[†] and Parukuttyamma Sujatha Devi [†£]

[†] Sensor and Actuator Division, CSIR-Central Glass and Ceramic Research Institute, Kolkata 700032, India, [£] CSIR- Network Institute of Solar Energy (CSIR-NISE), New Delhi, India.

Abstract: In view of the increased prospects of Zn_2SnO_4 as an alternative photoanode for dye sensitized solar cells (DSSC), we synthesized phase pure Zn_2SnO_4 nanostructures by a cost effective sonochemical technique. In order to establish the stability of this alternative photoanode in DSSC, we further explored the interaction of the synthesized Zn_2SnO_4 with commonly used photosensitizers in DSSC, such as N3, N719 and Eosin Y. Based on the time dependent optical studies we could establish the prominence of anchoring groups in controlling the dye loading. Optical studies confirmed an enhanced stable interaction of Zn_2SnO_4 with all the studied sensitizers which could be beneficial in designing DSSC devices in future. In addition, we also established contact angle as an indirect tool to understand the surface characteristics and thereby optimize the dye loading and stability of the photoanode surface. With the help of contact angle data, we could unequivocally establish the stability of Zn_2SnO_4 photoanode surface modified with N3 and N719 dye molecules. Our studies further suggest the enhanced and superior stability of the prepared Zn_2SnO_4 compared to ZnO in different chemical environments. The quenching of the fluorescence and the abrupt decrease in the contact angle owing to an increase in the surface roughness further strengthens the above conclusion. To our best knowledge, this probably is the first report on the synthesis of Zn_2SnO_4 by a sonochemical process and studies on its interaction with various photosensitizers. An exceptionally high open circuit voltage of >0.8V was observed for all the devices fabricated with the synthesized ZTO as photoanode. Our studies could pave way to the future developments in the area of DSSC using Zn_2SnO_4 as a photoanode.

Introduction

Dye sensitized solar cells (DSSC), a promising renewable energy source, have actively been investigated since its invention by Gratzel and coworkers in the early 1990s.[1] The lacunae of commonly used photoanodes such as ZnO, TiO_2 and SnO_2 and the necessity of identifying new photoanodes have generated great interest in exploring various multication oxides as alternative photoanodes in DSSC.[2] Interestingly, multication oxides, have the capability to integrate multiple functions in one system in addition to having the scope of tuning the physical and chemical properties by altering the compositions. Among the widely available multication oxides, Zn_2SnO_4, a ternary complex oxide (II-IV-VI oxide), acknowledged for its high electron mobility, high electrical conductivity, attractive optical properties has recently been investigated as a promising alternative photoanode to TiO_2 in DSSC.[3-5] The Zinc Stannate (ZTO) is an important n-type semiconducting oxide with an inverse spinel structure having *Fd3m* space group. This mixed oxide exhibits high electron mobility (10-15 $cm^2 V^{-1} s^{-1}$), high electrical conductivity, adequate thermodynamic stability and low visible absorption with a band gap of 3.6eV.[6] Interestingly, Zn_2SnO_4 also exhibits better properties than its binary counterparts ZnO and SnO_2.[7] Several wet chemical methods have been developed in recent years to prepare Zn_2SnO_4, the most important ones being electrospinning,[8,9] and hydrothermal reaction and utilized it for DSSC appliactions.[10-14] Here, we report a cost effective and scalable technique to prepare phase pure Zn_2SnO_4 nanostructures by a sonication induced precipitation method followed by annealing at 1000 ^oC for 8h.

In a typical DSSC device, semiconducting metal oxide, sensitizer dye and metal oxide/sensitizer/redox electrolyte interface are the three major components that determine the overall performance of the device. Despite the optimization of several other essential parameters, chemical stability of the metal oxide at the dye/metal oxide interface which

controls the electron injection and transport characteristics are still in the forefront of the research in this area. Various studies reported the vulnerable nature of ZnO in acidic environments resulting in the formation of Zn^{2+}/dye aggregates during sensitization.[3,14-17] In general, the dye loading on a photoanode depends on the nature and number of anchoring groups of the dyes in addition to the surface characteristics of the photoanode.[5,14,15,18,19] In order to increase and optimise the photochemical performance of a DSSC device, it is necessary to have effective and maximum dye loading on the photoanode without the formation of dye aggregates during adsorption. However, it is not always easy to fabricate a device and evaluate its performance for optimising the dye loading conditions.

Though there are many reports on the performance of Zn_2SnO_4 in DSSC, the studies pertaining to the stability of this important photoanode towards various dye molecules have not been carried out. Moreover, most of the available reports on ZTO in DSSC are with N719 dye molecule, very few with N3 and almost none with Eosin Y.[3-5, 10-14] In the pursuit for enhancing the efficiency, the researchers have overlooked the necessity to understand the stability of photoanodes in the chemical environment of inorganic sensitizers. It is essential to know the stability of this component in various chemical environments in order to excel their maximum potential in DSSC. Therefore, our focus was directed towards understanding the stability of Zn_2SnO_4 during its interaction with diverse inorganic sensitizers used in the DSSC device performance. For this purpose, three commonly used sensitizers viz. N3, N719 and Eosin Y exhibiting different acidity and pH values of 3.2, 5.6 and 7.7 respectively, in ethanol solution have been selected. More importantly, in addition to utilizing the spectroscopic techniques for evaluating the dye adsorption and stability, we have also explored the surface wettability of the films to understand the dye loading and stability aspects of the photoanode.

Materials and Methods

Materials

Zinc chloride [$ZnCl_2$ dry purified, 98%] from Merck, India, Tin(IV) chloride pentahydrate [$SnCl_4.5H_2O$, 98%] from Sigma Aldrich, Ammonia solution [~30% GR] from Merck, India, N719 dye [QN719 P64] from DYESOL, Australia, N3 and Eosin Y disodium salt from Sigma Aldrich, were used for the synthesis. The chemicals have been used as received. Double distilled water was used for synthesis. The Ethanol (absolute for analysis) used for the dissolution of the dyes was obtained from Merck, Germany.

Synthesis of phase pure Zn_2SnO_4

A controlled synthesis of pure Zn_2SnO_4 was achieved by ultrasonication (Rivotek, ultrasonic power 250 W, ultrasonic frequency 25 kHz, SS probe diameter 25 mm) followed by calcination. In a typical synthesis, 0.01 (M) Zinc chloride and 0.005 (M) Tin(IV) chloride pentahydrate were dissolved in 200 ml deionizer water under constant stirring for 15 minutes maintaining the final mole ratio of Zn^{2+} and Sn^{4+} as 2:1. Ammonia solution (30% GR) was added drop-wise to the mixture to main a final pH of 9 for precipitation resulting in a slurry like white precipitate. The solution containing precipitate was further sonicated repeatedly for four times (15 minutes) at a regular interval of 10 minutes. The precipitate was collected by filtration and washed with distilled water several times make it chloride free followed by drying under IR lamp around 70 ^oC for 4 hrs. Considering the mass loss in percentage from the thermal analysis, the as synthesized powder was calcined for 8hrs at 600 ^{o}, 800 ^{o}, 900 ^{o} and 1000 ^oC, respectively, at a heating rate of 100 ^oC/h. The fabricated films of the prepared Zn_2SnO_4 having thickness of ~ 8 μm and active area of 0.25 cm^2 were dipped in 0.5 mM N3, N719 and Eosin Y dyes in ethanol solution for overnight at room temperature. The films were taken out from the dye solutions with certain intervals and the UV-Vis absorption spectra of

the unadsorbed dye solutions were successively measured to monitor the dye adsorbing capability. The details of the film fabrication procedure have been reported elsewhere.[20] Ethanol dispersions of the prepared Zn_2SnO_4 of different concentrations starting from 0.5×10^{-2} M to 10×10^{-2} M have been mixed with ethanol solution of 0.5 mM N3, N719 and Eosin Y. The absorption spectra of the Zn_2SnO_4-dye conjugate solutions were measured after 12 hrs to understand the chemical stability. Similar experiments were performed with ZnO rods, at a shorter duration of 2hrs. The details of the preparation of ZnO rod and its characteristics have been reported elsewhere.[20, 21]

Material characterization

Thermo gravimetric analysis (TGA) and differential scanning calorimetric (DSC) studies of the as synthesized dried powder sample were carried out from RT to 1200 °C with a heating rate of 10 °C/ min on a NETZSCH 449C simultaneous thermal analyser to understand the thermal decomposition nature and thereby confirm the phase formation temperature. The dried powders were characterized for structural properties by powder X-ray diffraction (XRD) analysis on a X'pert pro MPD XRD of PAN analytical with Cu K_α radiation (λ=1.5406 Å). The X-ray diffraction measurement of the powder sample was further carried out at the Indian beamline (18B) in Photon Factory (PF), KEK, Japan. The energy of the synchrotron radiation used was set to 11.38 KeV (λ=1.089Å) for the scattering measurement. The elemental mapping and morphology of the powders were monitored on a scanning electron microscope (SEM), (LEO 430i, Carl Zeiss). Morphology of the same were further monitored using transmission electron microscopy (TEM) which was carried out on a Tecnai G2 30ST (FEI) high resolution transmission electron microscope operating at 300 kV. Fourier transform infrared (FTIR) absorption spectra of the samples were recorded on a Nicolet 380 FTIR spectrometer using KBr in order to confirm the formation of pure ZTO phases with increasing temperature. Raman spectra were collected on a Renishaw InVia

Reflex micro Raman spectrometer with excitation of argon ion (514 nm) lasers. The spectra were collected with a resolution of 1 cm^{-1}. The cross-sectional FESEM images of the coated films were checked on a Field Emission Scanning Electron Microscope (Supra 35VP, Carl Zeiss). To optimize the duration for maximum loading the optical absorption spectra of the unadsorbed dye solutions have been measured on a UV-Vis-NIR spectrometer (Shimadzu UV-3600). The diffuse reflectance (DR) spectra before and after dye loading for 24 hrs were also measured subsequently. The absorption spectra of the dyes in ethanol solution, ethanolic dispersion of Zn_2SnO_4 and ZnO and dyes after adsorption on Zn_2SnO_4 and ZnO films were measured to establish the comparative stability of the metal oxides. The room temperature fluorescence spectrum of colloidal Zn_2SnO_4 and ZnO solutions were performed on a steady state spectrofluorometer (QM-40, Photon Technology International, PTI) using a Xenon lamp as an excitation source, at an excitation wavelength of 525 nm and band pass of 5 nm. The comparative surface wettability of the films of the Zn_2SnO_4 particles and ZnO rods sensitized with N3 and N719 at different sensitization times were accomplished by measuring the successive water contact angles on a Drop Shape Analyzer (Kruss DSA25) using the Young's equation (sessile drop method). The volume of each drop was fixed at 5 μL and the dosing rate was 500 μL/min. The instrument was equipped with a CCD camera for image capture.

Fabrication of the dye-sensitized solar cell

The ZTO films were fabricated by the doctor blade method on FTO glass (7 Ω/ cm^2) followed by annealing at 450 °C for 1 h. The thickness of ZnO films were maintained ~8 μm. The 0.5 mM solution of N3, N719 and Eosin Y dye in ethanol were used as the sensitizers. The I−V characteristics were measured using a solar simulator (Newport) at 100 mW/cm^2 (1 sun AM 1.5). Standard silicon solar cell (SER NO. 189/PVM351) from Newport, U.S. was used as a reference cell. The data presented are an average of measurements taken on two different devices for each sample.

Results and Discussion

Structural and micro-structural studies

In order to understand the thermal decomposition behaviour of the as-prepared powder, we have carried out the thermogravimetric analysis of the samples. The TG graph (Fig. 1a) of the as-prepared powder exhibited a total weight-loss of 19.66 wt. % within room temperature to 1200 °C having three discernible steps at around 50, 150 and 800 °C, respectively.

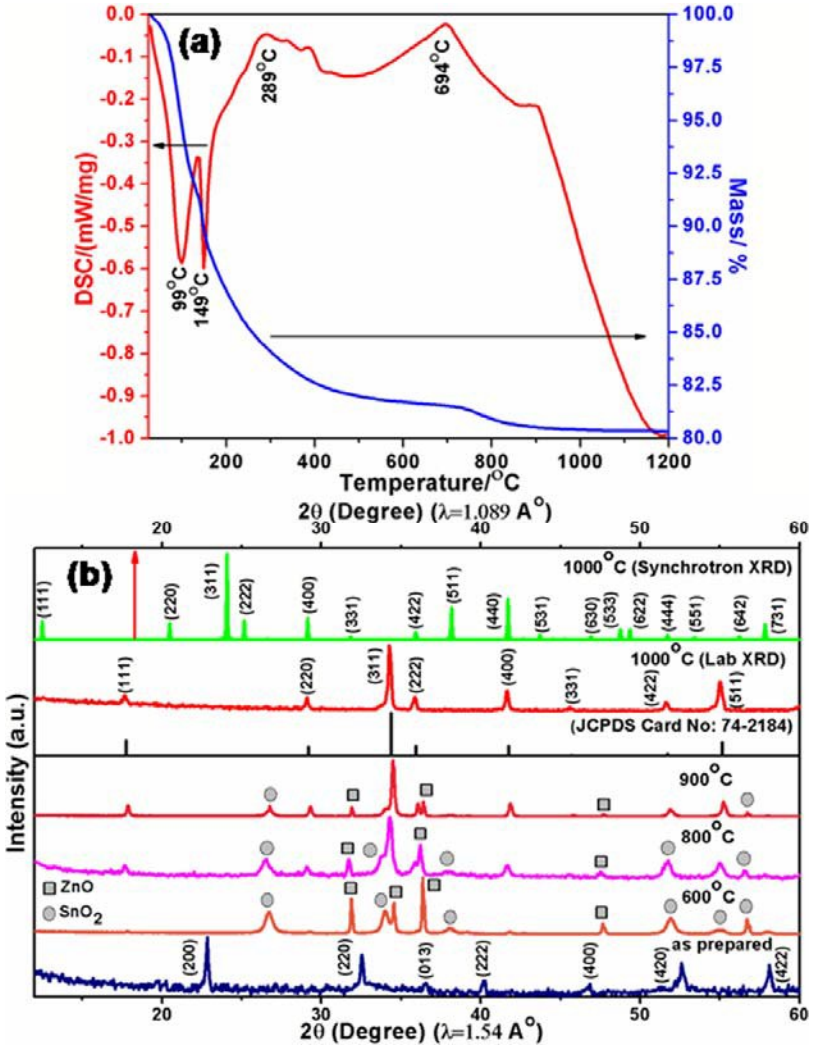

Fig. 1 (a) The TG-DSC curves of the as synthesized precursor of Zn_2SnO_4 and (b) XRD patterns of as synthesized precursor and that calcined at 600 °, 800 °, 900 °, and 1000 °C,

respectively, for 8h and the synchrotron X-ray diffraction pattern of the 1000 ^{o}C/8h calcined sample.

On the other hand, the DSC curve revealed two endothermic peaks at about 99 and 149 °C and two exotherms at about 289 and 694 °C, respectively. The thermal analysis results suggest that the initial endotherms in the DSC curve and the initial weight loss steps in the TG curve are characteristics of the desorption of surface-adsorbed water, and NH_4^+ ions, respectively. The most salient weight loss in the third step of the TG curve could be attributed to the decomposition of the hydroxide, $ZnSn(OH)_6$, with the consequent formation of a mixture of thermodynamically stable phases ZnO and SnO_2. This corresponds to a broad exotherm in the DSC curve at about 289 °C. The crystallisation of Zn_2SnO_4 beyond 500 °C is evidenced by the appearance of a broad exotherm at about 694 °C in the DSC curve.

The X-ray powder diffraction (XRD) pattern shown in Fig. 1(b) confirms that after the immediate addition of base to the precursor solution lead to the formation of $ZnSn(OH)_6$, which is in good agreement with the standard values reported in the JCPDS file no: 73-2384 for the same. The formation of $ZnSn(OH)_6$ is attributed to the following reaction shown in eqn (1).

$$Zn^{2+} + Sn^{4+} + 6\ OH^- \longrightarrow ZnSn(OH)_6 \downarrow \quad \text{..... (1)}$$

Most of the diffraction peaks of the calcined $ZnSn(OH)_6$ starting from 600 ^{o}C to 900 ^{o}C has been preferably indexed to a combination of cubic spinel Zn_2SnO_4, hexagonal ZnO (JCPDS 36-1451) and tetragonal SnO_2 (JCPDS 72-1147) phases in different proportions. This further supports the rapid mass loss in the third step of the TGA graph which can be represented by the following reaction in eqn (2).

$$3\ ZnSn(OH)_6 \longrightarrow ZnO + 2SnO_2 + Zn_2SnO_4 + 9H_2O \uparrow \quad \text{.....(2)}$$

The XRD pattern of the sample prepared by calcining the as synthesized $ZnSn(OH)_6$ at 1000 ^{o}C exactly matches with the reported reference pattern of inverse cubic spinel Zn_2SnO_4

(JCPDS 74-2184) thus confirming the formation of phase pure Zn_2SnO_4 at this particular temperature. This data further corroborates the thermal analysis data shown in Fig. 1(a). In order to ascertain the presence of any impure phase in the final product, we have carried out high resolution XRD measurements using the synchrotron X-ray diffraction with an energy of 11.38 KeV (λ=1.089Å). The synchrotron data unequivocally confirms the phase purity of the prepared Zn_2SnO_4. The formation of Zn_2SnO_4 is believed to occur by the following reaction displayed in equation (3).

$$2\ ZnO + SnO_2 + Zn_2SnO_4 \longrightarrow 2Zn_2SnO_4 \ldots\ldots\ldots (3)$$

The calculated lattice parameter of the prepared phase pure Zn_2SnO_4 is a=8.723 Å which is comparable to the reported lattice constant a=8.650 Å of the cubic Zn_2SnO_4.

We have also monitored the formation of Zn_2SnO_4 from the thermal decomposition of $ZnSn(OH)_6$ by FT-IR spectroscopy. The FT-IR spectra of the as prepared $ZnSn(OH)_6$ and that calcined at 600 °, 800 °C and 1000 °C, respectively, are presented in Fig. 2(a).

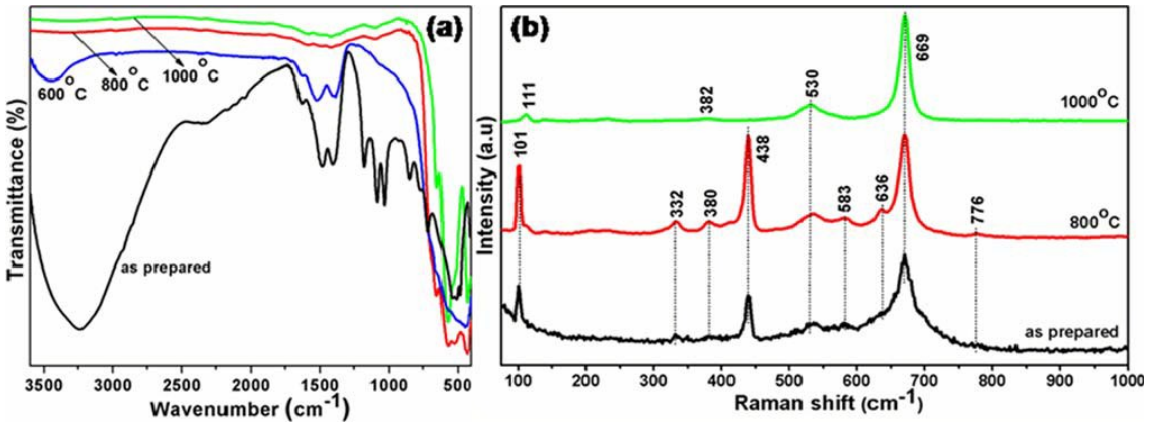

Fig. 2 (a) FTIR and (b) Raman spectra of as prepared $ZnSn(OH)_6$ and that calcined at 600 °, 800 ° and 1000 °C, respectively.

A strong and broad absorption peak in the range of 2500-3600 cm^{-1} centred at 3235 cm^{-1}, corresponds to the stretching vibration of O-H bonds of the hydroxyl groups present in the as synthesized $ZnSn(OH)_6$. The corresponding bending mode appeared at 1634 cm^{-1}.These peaks

gradually disappear with increase in the calcination temperature, indicating the removal of water on decomposition. The same trend was also observed for the peaks around 1404 and 1485 cm^{-1} corresponding to the adsorbed NH_4^+ groups. The bands at 1033, 1087 and 1180 cm^{-1} appearing in the IR spectrum of the as-prepared sample could be attributed to the vibrations of M-OH or M-OH-M bonds of $ZnSn(OH)_6$, where M corresponds to Zn and Sn. Generally, the IR active vibrational modes for SnO_2 predominantly appear at 667 and 616 cm^{-1}. On the other hand, the bands at 530, 495 and 440 cm^{-1} are the typical vibrational modes of ZnO. The weak bands appeared around 663, 572 and 440 cm^{-1} correspond to the respective vibrational bands of SnO_2, Zn_2SnO_4 and ZnO, thereby suggesting the distinct presence of all the three phases in the sample calcined at 600 °C. This further confirms the nucleation of the Zn_2SnO_4 phase at 600 °C. Relevant changes in the FT-IR spectrum were observed for the sample calcined at 800 °C as well. The band appearing at 572 cm^{-1} assigned to the Zn_2SnO_4 spinel phase became more eminent and relevant shift in the vibration bands for Sn-O and Zn-O bonds were also observed on further increase in the calcination temperature. It is worth mentioning the characteristic vibration band for Sn-O-Zn bond of the Zn_2SnO_4 which appeared at 572 cm^{-1} becoming more predominant by calcining at an elevated temperature of 1000 °C.[22] The IR results also confirms the formation of pure Zn_2SnO_4 at 1000 ^oC.

In order to further assess the structural quality of the prepared samples, we have carried out the Raman spectroscopic analysis of as synthesized $ZnSn(OH)_6$ and calcined samples with 514 nm Ar+ laser at room temperature as presented in Fig. 2(b). The fundamental Raman scattering peaks appeared in the calcined samples 600 ^{o} and 800 ^oC confirmed the existence of a mixture of ZnO and SnO_2 along with Zn_2SnO_4 in different proportions. The intense peak appeared at 438 cm^{-1} corresponds to the intrinsic Raman-active E2 mode characteristic of the hexagonal wurtzite phase of ZnO. The peak at 332 cm^{-1} corresponds to the multi-phonon scattering processes whereas the E1 (LO) mode at 583 cm^{-1} corresponds to the presence of

defects such as oxygen vacancies or oxygen interstitial in ZnO.[20] The characteristic Raman scattering peaks for tetragonal SnO_2 phase were also observed at 636 cm^{-1} and 776 cm^{-1} attribute to the A1g and B2g vibration modes, respectively.[23] The remaining peaks signify the characteristic Raman active modes of Zn_2SnO_4. The only intense peak at 669 cm^{-1} of A1g symmetry corresponds to the typical Raman shift of Zn_2SnO_4 which is associated with the symmetric stretching of the Zn–O bonds in the ZnO_4 tetrahedra of the inverse spinel Zn_2SnO_4 appeared at 1000 ^oC annealed sample.[11] In addition, the other phonon modes at 532 cm^{-1} and 382 cm^{-1} assigned to the F2g(1) and F2g(2) symmetries, respectively, correspond to the symmetric and asymmetric bending of oxygen atoms in the M–O bonds of the MO_6 octahedra (M = Zn or Sn). The characteristic Raman active modes of ZnO and SnO_2 were interestingly absent in these samples thereby confirming the formation of Zn_2SnO_4 at 1000 ^oC. [11, 24]

The SEM image shown in Fig. 3(a) exhibits an overview of the morphology of the prepared phase pure Zn_2SnO_4.

Fig. 3 (a) The FESEM image of pure Zn_2SnO_4, (b) line scanning mapping analysis from a

selected area of the sample and (c) to (e) represents the elemental mapping from a selected area, (f) bright field TEM image, (g) HRTEM, (h) SAED pattern. Inset shows FFT of the HRTEM.

It could be clearly seen that the material is composed of uniform sized particles with a mean diameter of 100-125 nm. This observation suggests that the present solution route could be a facile method for the large scale synthesis of uniformly sized phase pure Zn_2SnO_4 particles. To our knowledge this probably is the first report on the synthesis of Zn_2SnO_4 by sonochemical process. To understand the elemental distribution of Zn, Sn and O in the prepared Zn_2SnO_4, the elemental mapping over a selected line of 7 micron and over a large area had been performed using FESEM (EDX) analysis (Fig. 3b). Almost a homogeneous and uniform distribution of all the elements, Zn, Sn and O, were observed throughout the selected line of the prepared Zn_2SnO_4. The large area mapping also equally exhibited highly dispersed nature of each element throughout the material. These are displayed in Fig. 3(c-e), respectively. For further investigation of the morphology and crystallinity of the prepared Zn_2SnO_4, the TEM images were recorded as shown in Fig. 3(f-h). The bright field TEM image shown in Fig. 3(f) corroborates with the size and shape of the particles obtained from FESEM images. The high-resolution TEM image in Fig. 3(g) further confirms the single crystalline nature of the synthesized Zn_2SnO_4 particles with the line spacing corresponding to the (111) reflection. The SAED pattern in Fig. 3(h) indicates the (111), (222), (511), (444), (400) and (311) planes and the inset of 3(g) exhibits the corresponding FFT of the particular HRTEM.

In order to monitor the optical properties of the synthesized Zn_2SnO_4, UV-Vis absorption and emission measurements were performed on the 1000 ^oC calcined sample (Figure not shown). The optical absorbance for the intrinsic band gap transition of the 1000 ^oC calcined sample

was observed around 325 nm corresponding to a band gap of 3.7 eV following the Tauc's formula.

Adsorption properties of Zn_2SnO_4 films towards the sensitizers N3, N719 and EosinY

In order to understand and establish the stability of the Zn_2SnO_4 in the chemical environment of sensitizers exhibiting different acidity, three commonly used dyes viz. N3, N719 and Eosin Y exhibiting pH values of 3.2, 5.6 and 7.7, respectively, in solution have been selected for our study. The relative stability of the Zn_2SnO_4 has also been compared with ZnO, which is believed to be unstable under acidic pH conditions. As both the metal oxides have been prepared in a strongly basic medium (pH ~ 9) the chemical stability has been selectively monitored from neutral to acidic environments. For this purpose we have chosen, N3 dye molecule having four free carboxylic acid groups (-COOH), N719 with two and Eosin Y with one carboxylic and one hydroxyl groups for anchoring. In order to study the dye adsorbing capability, the prepared films having thickness of ~ 8 μm and active area of 0.25 cm^2 were immersed in 0.5 mM N3, N719 and Eosin Y in ethanol for different duration of time at room temperature. After adsorption for a definite duration, the films were taken out from the dye solutions and the UV-Vis absorption spectra of the unadsorbed dye solutions have been successively measured. Fig. 4(a) represents the concentrations of the unadsorbed Eosin Y, N719 and N3 dye solutions as a function of time. Here, it is evident that the concentration of the remaining dye solution exponentially decrease in the order N3> N719>>Eosin Y with time with N3 showing maximum decrease and adsorption of dye molecules. It could be clearly observed that the process of dye loading was rapid for the first few hours for all the dyes (Fig. 4a). On preceding the adsorption process, interestingly, a saturation of adsorption was noticed for all the dyes depending on the chemical nature of the dyes. The N3 dye having

four carboxylic groups took more time to get saturated compared to N719 having two carboxylic groups. On the contrary, the adsorption of the Eosin Y having only one carboxylic and hydroxyl group as anchoring groups achieved saturation at a shorter duration of time.

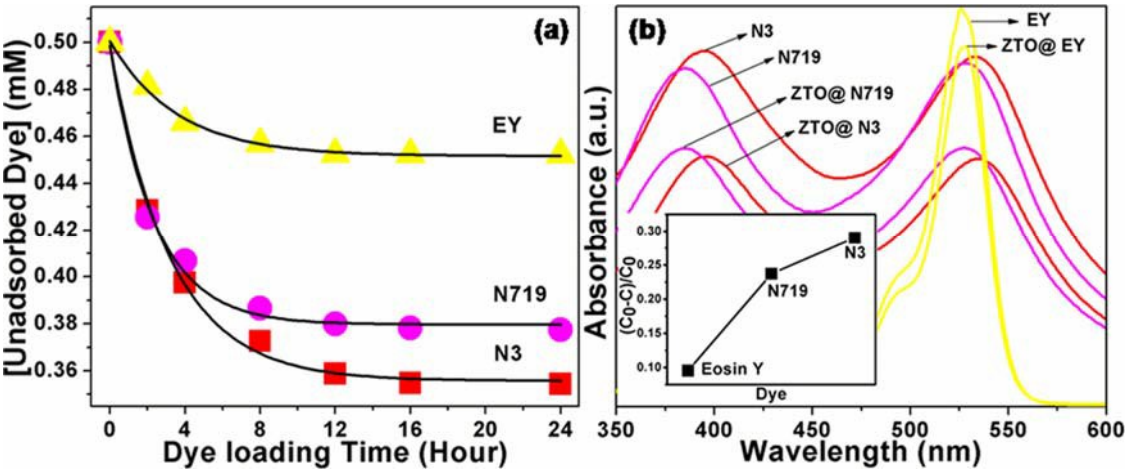

Fig. 4 (a) The concentrations of the unadsorbed Eosin Y, N719 and N3 dye solutions as a function of time and (b) UV-Vis absorption spectra of initial N3, N719 and Eosin Y dye solution in ethanol and the corresponding unadsorbed dye solution after 24 hours. The inset shows the (C*o*-C)/C*o* data calculated for all the three dye molecules.

Fig. 4(b) represents the absorption spectra of the N3, N719 and Eosin Y dye solution in ethanol before and after loading for 24 hrs. The percentage of the dye adsorbed by the Zn_2SnO_4 films could be expressed by the formula (C*o*-C)/C*o*, [25] where C*o* is the initial concentration of the dyes and C is the concentration of the residual dye in solution considering the respective absorbance values at 537, 527 and 528 nm for N3, N719 and Eosin Y, respectively. It can be calculated that the dye adsorption ability, (C*o*-C)/C*o* is in the order of Eosin Y<<N719< N3 as clear from the inset graph shown in Fig. 4(b). This study confirms that the amount of dye loading on the Zn_2SnO_4 films, interestingly follows the order of increasing anchoring groups as one carboxyl and hydroxyl<<two carboxyl<four carboxyl groups.

Photophysical properties of the dyes with Zn_2SnO_4 and ZnO powder dispersions

To investigate the stability of the prepared Zn_2SnO_4 in presence of different dye solutions, we have mixed the dyes with homogeneous dispersion of the metal oxide powder in ethanol. For this purpose, 0.5 mM each of N3, N719 and Eosin Y solutions were mixed with Zn_2SnO_4 dispersions of different concentrations staring from 0.5×10^{-2} M to 10×10^{-2} M. The Zn_2SnO_4-dye conjugate solution has been kept intact for 12 hrs which is the average saturation time for absolute dye loading. The same experiments were also carried out with ZnO rods, but at a shorter duration of 2h. The corresponding absorption spectra of the dye solution in presence of Zn_2SnO_4 and ZnO dispersions are respectively, presented in Fig. 5(a), (c), (e) and (b), (d), (f). Interestingly, the absorption maxima of the neutral Eosin Y remained unchanged in presence of both the metal oxides as revealed in Fig. 5(a) and (b). However, a distinct and gradual blue shift in the absorption maxima of the most acidic N3 dye was observed with

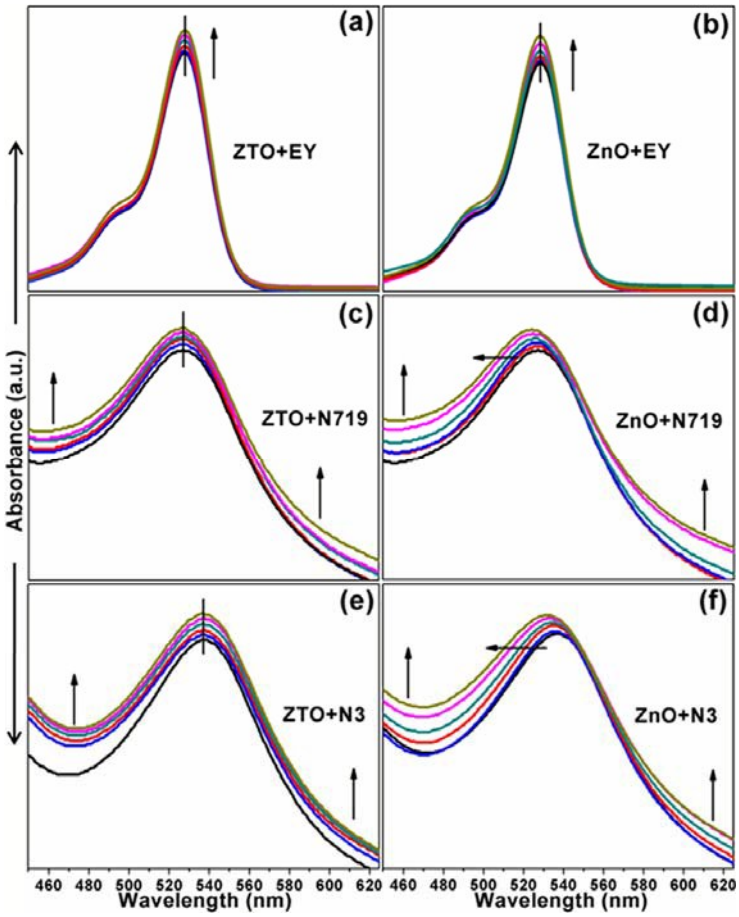

Fig. 5 Absorption spectra of (a) and (b) Eosin Y, (c) and (d) N719, (e) and (f) N3 (0.5 mM) in ethanolic dispersion of Zn_2SnO_4 particles and ZnO rods, respectively at varied concentrations of 0, 0.5×10^{-2}, 1×10^{-2}, 2.5×10^{-2}, 5×10^{-2} , and 10×10^{-2} M.

increase in the concentration of ZnO whereas the moderately acidic N719 dye exhibited a marginal shift in the absorption maxima. This is due to the fact that with simultaneous increase in the acidity of dyes as well as the concentration of ZnO, the formation of Zn^{2+}/dye aggregates occurs resulting in a blue shift in the absorption maximum. The minor increase in the absorption spectra can be attributed to the scattering effect induced by the increment in the concentration of the metal oxide powder. On contrary to the behavior of ZnO, there was insignificant or no shift in the absorption maxima of the dyes on interaction with Zn_2SnO_4. This strongly suggests the absence of dye aggregates formation in presence of Zn_2SnO_4 and ascertains the better stability of the prepared Zn_2SnO_4 especially in acidic environment. This could, in actual device, can result in an increment in the photocurrent as less aggregation makes the dye more active for electron injection and further restricts the probability of making blockage into the pores of the photoanode matrix which increases the interpenetrating ability of the electrolyte and substantially may increase the overall cell efficiency of the DSSCs device.[14] This information could be highly useful in the choice of dye molecules for DSSC device fabrication and optimization.

Photophysical properties of the dyes adsorbed on Zn_2SnO_4 and ZnO films

To further establish the better chemical stability of the prepared Zn_2SnO_4 particles than ZnO, we have extended the dye interaction study for the films also. The cross sectional FESEM images of the ZTO and ZnO coated films have been shown in Fig. S1. The measured thicknesses were 8.75 and 8.68 μm, respectively, for ZTO and ZnO films. The films have been selectively immersed into the most acidic N3 dye solution of 0.5 mM for 12 hrs for

Zn_2SnO_4 and 2 hrs for ZnO. The absorption spectra of the dye adsorbed films have been measured as shown in Fig. S2(a). Compared to the original band maximum of N3 at 537 nm, the absorption maximum of N3 adsorbed on ZnO films remarkably shifted towards blue region by 11-12 nm whereas a negligible shift of only 0.5-1 nm was observed for N3 adsorbed on the Zn_2SnO_4 film surface. This result further confirms the better stability of Zn_2SnO_4 films on interaction with acidic dye by preventing the formation of dye aggregates for a longer duration of time. It can also be inferred that the porosity, roughness and larger surface area of the films make allowance for more amount of dye to adsorb compared to the powder dispersion. This could probably result in the formation of more aggregation between the metal oxides and dye molecules leading to a larger shift in the absorption spectra of the acidic dye N3 (Fig. S2a).

Effect of dye aggregation; quenching of emission

To further disclose the formation of Zn^{2+}/dye aggregates with ZnO, the room temperature emission spectra of Zn_2SnO_4 and ZnO dispersed in 0.5 mM N719 ethanolic solution were monitored as shown in Fig. S2(b). Here, also the interaction duration has been fixed at 12 hrs for Zn_2SnO_4-N719 and 2 hrs for ZnO-N719 dispersion. The spectra have been recorded under 525 nm light excitation. The N719 dye in ethanol exhibited two distinct emission peaks at around 760 and 798 nm. A drastic quenching in fluorescence has been observed for N719 in ZnO dispersion. The quenching on the other hand was negligible in Zn_2SnO_4 dispersion. This further verifies the formation of dye aggregates resulting in quenching of the fluorescence in the presence of ZnO.

Diffuse reflectance measurements

Based on the spectroscopic analysis on the interaction of various dye molecules with Zn_2SnO_4, a schematic has been presented in Fig. 6(a) to highlight the possible ways of interaction of various functional groups present in the dye molecule. Due to the presence of

three carboxylic functional groups in N3, its interaction with Zn_2SnO_4 is expected to be better compared to others. The extent of loading of the dye molecules by ZTO particles were further determined by the diffuse reflectance (DR) spectra of the Zn_2SnO_4 films before adsorption and after impregnation for 24 hrs at room temperature (Fig. 6b). An abrupt decrease in reflectance at around 325nm corresponds to the inter-band absorption of Zn_2SnO_4. The dye loaded Zn_2SnO_4 also exhibited an additional broad absorption band between 750 nm to the UV region of the electromagnetic spectrum due to electronic excitation of the adsorbed dyes. The shape of the spectrum corresponds to that of the absorption spectrum of the adsorbed dyes. The low reflectance of dye loaded Zn_2SnO_4 indicates successful loading of dyes on the Zn_2SnO_4 surface which is crucial for DSSC device performance. [20] The reflectance from the Zn_2SnO_4 film surface varied in the order, Eosin Y>> N719> N3 which again appears to depend on the anchoring groups of the dye molecules and strongly corroborates the UV-Vis spectroscopic studies for monitoring the extent of dye loading (Fig. 4).

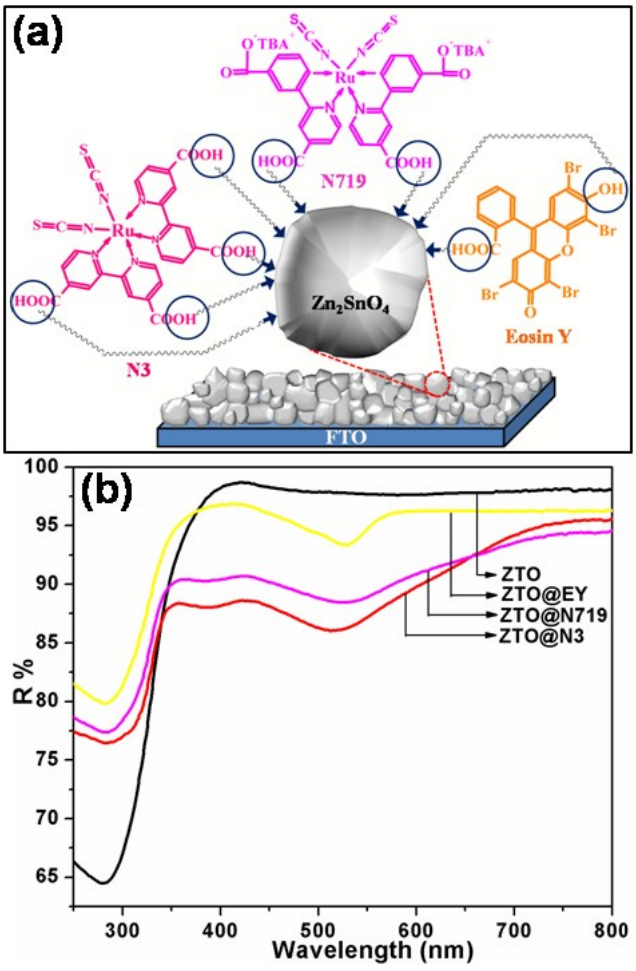

Fig. 6 (a) A schematic illustration of the possible interactions of metal oxide (Zn_2SnO_4)/dye (N3, N719 and Eosin Y), and (b) Diffuse reflectance spectra of synthesized Zn_2SnO_4 film and N3, N719 and Eosin Y dye loaded Zn_2SnO_4 film.

Surface characteristics through contact angle measurement

The change in surface characteristics of the films before and after dye loading, have been monitored by measuring the contact angle (CA) which is a unique technique to understand the surface properties. The shape of liquid droplets falling on the solid surface is a direct way to understand the wettability of the surface. The behaviour of a water droplet on the film surface was thus monitored as shown in Fig. 7(a).

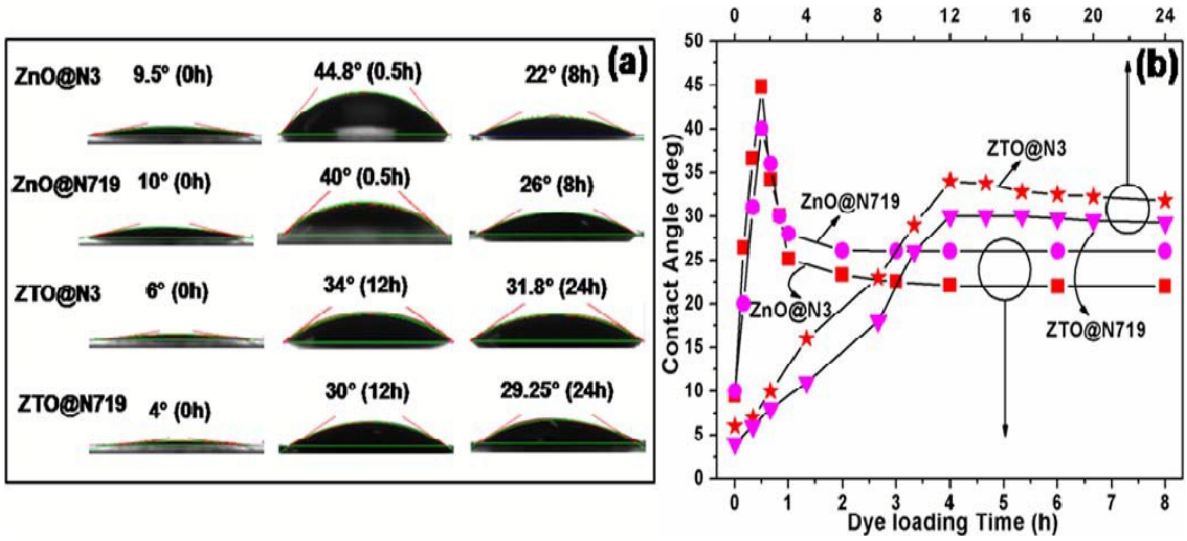

Fig. 7 (a) Images of water droplets on the film surface, (b) contact angle measurements of N3 and N719 adsorbed ZnO rods and synthesized Zn_2SnO_4 particles films surface as a function of dye loading time.

The elliptical nature of the droplet size is an indication of the hydrophilic nature of the surface. The measured contact angle as a function of dye loading time is plotted in Fig. 7(b). Here, we have compared the surface characteristics of N3 and N719 adsorbed ZnO and ZTO films. Both the films without dye loading exhibited contact angles of below 10 °

characteristics of super hydrophilicity of the films. The ZnO films sensitized with N3 dye solution for 30 minutes, interestingly, exhibited a substantial increase in contact angle to ~ 44 °. This indicates a successful adsorption of the N3 dye molecules onto the ZnO film surface. The corresponding contact angle was ~ 40 ° for N719 further supporting its weaker adsorption capability compared to N3. With increase in the dye loading time for one hour, the contact angle abruptly reduced to ~ 25 ° for N3 and ~ 28 ° for N719, respectively. This is attributed to the change in the surface characteristics of the ZnO film. The formation of the inhomogeneous Zn^{2+}/dye complex on the surface changes the surface properties from comparatively hydrophobic to hydrophilic in nature. The relatively lower contact angle of the acidic N3 surface compared to N719 after 1 hr loading is due to the formation of more Zn^{2+}/dye aggregates in presence of the former compared to the later. This further, underscores the reason for a blue shifting of N3 in ZnO dispersion during the absorption study. In contrary to the results of ZnO films, a gradual increase in the contact angle upto 12 hrs was observed for the prepared Zn_2SnO_4 films starting from ~ 4-6 ° to ~ 30-34 ° by loading with N719 and N3 dyes due to the successful adsorption of the dye molecules. The contact angle values interestingly remained almost constant up to 24 hrs of sensitization time. There was no change in the contact angle after 12hrs confirming the saturation of dye adsorption on the surface with no dye aggregates formation at the Zn_2SnO_4/dye interface.[26] The variation of contact angle with sensitization time indicates a good correlation with the stability of the dye molecules in presence of the photoanode. Ambade et al., have used contact angle measurement as an empirical diagnostic method to pre-evaluate the performance of ZnO based DSSC for the first time.[26] Here, we have used CA measurements to unequivocally establish the stability of Zn_2SnO_4 photoanode surface modified with N3 and N719 dye molecules.

The photophysical properties of the studied materials are summarized in Table 1.

Table 1 Photophysical properties of Eosin Y, N3 and N719 in ethanol and the same adsorbed on Zn_2SnO_4 powder and films.

	Eosin Y	N719	N3
pH in ethanol	7.7	5.6	3.2
λ^{ab}_{max} in ethanol/ nm (main peak under our observation)	528	527	537
Amount adsorbed per unit area of the Zn_2SnO_4 film (mM/cm^2)	0.191	0.474	0.58
Shif of λ_{max} in Zn_2SnO_4	insignificant	insignificant	insignificant
and ZnO solutions/nm		2-3	5-6
Shift of λ_{max} adsorbed on Zn_2SnO_4	insignificant	insignificant	0.5-1
and ZnO films of ~2 μm/nm		5-6	11-12

DSSC cell testing and performance

The performance of the fabricated devices with the synthesized Zn_2SnO_4 was further investigated by employing all the studied sensitizers from N719 to N3 to Eosin Y. According to the average saturation period for loading of the three different dyes with Zn_2SnO_4 [Fig. 4(a)] the dye sensitization time have been fixed at 8hrs and 12hrs for cell testing. The *J-V* characteristics of the fabricated DSSCs are shown as Fig. 8 and the corresponding photovoltaic properties are collated in Table 2.

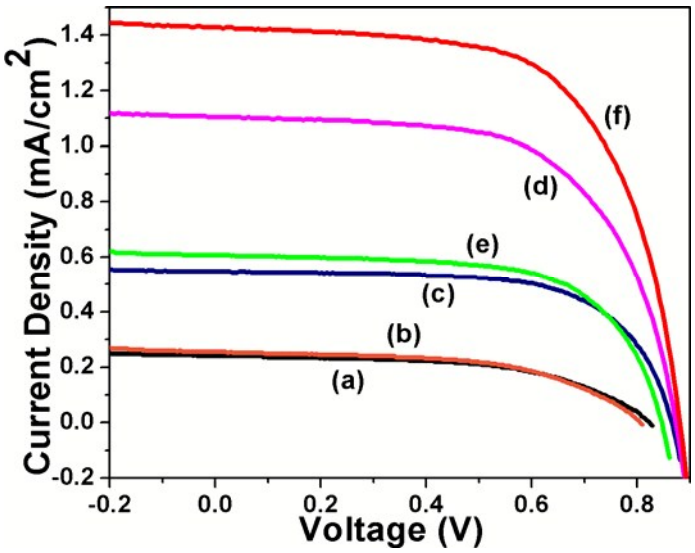

Fig. 8 *J-V* characteristics of fabricated DSSC with the synthesized Zn_2SnO_4 nanoparticles with dipping times of 8 and 12h, respectively: (a) & (b) Eosin Y, (c) & (d) N3 and (e) & (f) N719.

Table 2 Photovoltaic properties of the Zn_2SnO_4 using the sensitizers Eosin Y, N3 and N719 at two different dipping times.

Dye Used	Dipping Time (hrs)	V_{oc} (V)	J_{sc} (mA/cm^2)	FF (%)	η (%) ±0.02
Eosin Y	8	0.82	0.24	55.78	0.11
Eosin Y	12	0.81	0.25	54.96	0.12
N3	8	0.86	0.54	65.85	0.31
N3	12	0.87	1.11	62.28	0.61
N719	8	0.84	0.61	64.71	0.34
N719	12	0.88	1.43	63.49	0.81

Interestingly, an exceptionally high open circuit voltage of >0.8V was observed for all the devices which undoubtedly establish the synthesized Zn_2SnO_4 as a potential candidate for the DSSC application. A significantly lower J_{sc}, FF and efficiency were observed for Eosin Y which could be due to the poor adsorption ability of the same. A negligible improvement in the photovoltaic performance with increase in the sensitization time from 8hrs to 12hrs accounts for the saturation of adsorption of the dye around 8hrs (Fig. 4a). On the contrary, the J_{sc} and efficiency enhances with time for N719 and N3 dye due to the higher dye loading at 12hrs (Fig. 4a). Thus, the photovoltaic properties of the synthesized Zn_2SnO_4 are in compliance with its dye loading behavior exhibited in Fig. 4a. No significant difference in the performance of the fabricated devices using N719 or N3 as sensitizers, have been observed which further highlights the stability of the Zn_2SnO_4. Interestingly the minor increment in the J_{sc} and efficiency for the fabricated devices using N719 compared to N3 at longer sensitization times of 12hrs eventually emphasizes the influence of stability of photoanode with sensitizer as a predominating parameter over the amount of dye loading for better

performance of DSSCs. In all the cases, the observed efficiency was very low than expected for this system. Further experiments in optimizing the concentration of dye molecules and the thickness of the photoanode films are underway to exploit the utilization of the synthesized ZTO as an efficient photoanode in DSSC.

Conclusions

A sonication assisted precipitation process was employed to prepare phase pure Zn_2SnO_4 nanostructures by annealing the as-prepared precipitate at 1000 ^oC for 8hrs. Taking into consideration of the prospects of Zn_2SnO_4 as a potential alternative photoanode for DSSC, in this study, we have explored the interaction of different photosensitizers with Zn_2SnO_4. Based on the time dependent optical studies it can be concluded that the amount of dye loading of the prepared Zn_2SnO_4 films was maximum for N3 and minimum for Eosin Y. The systematic physicochemical absorption studies further confirmed that the N3, N719 and Eosin Y dyes of different acidity undergo a very stable interaction with the prepared Zn_2SnO_4 and exhibited favorable binding onto the prepared Zn_2SnO_4 films surface for a much longer sensitization time than ZnO. This suggests that the prepared Zn_2SnO_4 is quite stable compared to ZnO which forms Zn^{2+}/dye aggregates in acidic environment. In this study, we have also used CA measurements to unequivocally establish the stability of Zn_2SnO_4 photoanode surface modified with N3 and N719 dye molecules. Our studies could pave way to the future developments in the area of DSSC using Zn_2SnO_4 as a photoanode. The preliminary results of the device performances based on the synthesized ZTO with different dyes elucidate the stability factor between the photoanode and sensitizer as the predominating parameter over the extent of dye loading. An exceptionally high open circuit voltage of >0.8V is observed for all the devices fabricated with the synthesized ZTO as photoanode using three different sensitizers. Further studies are in progress to monitor the performance of the DSSC device with the studied dye molecules.

Supporting Information

Cross-sectional FESEM images of ZTO and ZnO films, absorption spectra of the N3 and that adsorbed on ZnO film and Zn_2SnO_4 film, emission spectra of N719 in ethanol and that taken in 10×10^{-2} M Zn_2SnO_4 and ZnO dispersions in ethanol.

Acknowledgements

PSD acknowledges Ministry of New and Renewable Energy (MNRE) for financial support under the CSIR-TAPSUN program. PPD acknowledges financial support from MNRE for the fellowship to carry out the Ph.D program. AR thankfully acknowledges DST-INSPIRE program for junior research fellowship. The authors acknowledge the help rendered by Dr. S. B. Ogale, former scientist, CSIR-National Chemical Laboratory for providing the facilities created under CSIR-TAPSUN program for DSSC cell testing. PSD also acknowledges the central instrumentation facilities of CSIR-CGCRI for assistance. We also thank the reviewers for their critical comments on our manuscript, and providing useful and constructive suggestions for improving the scientific quality and presentation of the data in the manuscript.

Notes and References

1 B. Oregan and M. Gratzel, *Nature*, 1991, **353**, 737-740.

2 M. Ye, X. Wen, M. Wang, J. Iocozzia, N. Zhang, C. Lin and Z. Lin, *Materials Today*, 2015, **18**, 155-162.

3 B. Tan, E. Toman, Y. Li and Y. Wu, *J. Am. Chem. Soc*., 2007, **129**, 4162-4163.

4 T. L. Villarreal, G. Boschloo and A. Hagfeldt, *J. Phys. Chem. C*, 2007, **111**, 5549-5556.

5 J. Chen, L. Lu and W. Wang, *J. Phys. Chem. C*, 2012, **116**, 10841-10847.

6 T. J. Coutts, D. L. Young, X. Li, W. P. Mulligan and X. Wu, *J. Vac. Sci. Technol. A*, 2000, **18**, 2646-2660.

7 D. L. Young, H. Moutinho, Y. Yan and T. J. Coutts, *J. Appl. Phys*., 2002, **92**, 310-319.

8 S. H. Choi, I. S. Hwang, J. H. Lee, S. G. Oha and I. D. Kim, *Chem. Commun*., 2011, **47**, 9315-9317.

9 T. Lim, H. Kim, M. Meyyappan and S. Ju, *ACS NANO*, 2012, **6**, 4912-4920.

10 J. Wang, X. W. Sun, S. Xie, W. Zhou and Y. Yang, *Cryst. Growth Des***.,** 2008, **8**, 707-710.

11 V. Sepelak, S. M. Becker, I. Bergmann, S. Indris, M. Scheuermann, A. Feldhoff, C. Kubel, M. Bruns, N. Sturzl, A. S. Ulrich, M. Ghafari, H. Hahn, C. P. Grey, K. D. Becker, and P. Heitjans, *J. Mater. Chem*., 2012, **22**, 3117-3126.

12 H. Zhu, D. Yang, G. Yu, H. Zhang, D. Jin and K. Yao, *J. Phys. Chem. B*, 2006**, 110**, 7631-7634.

13 A. M. A. Alpuche and Y. Wu, *J. Am. Chem. Soc*., 2009, **131**, 3216-3224.

14 V. Thavasi, V. Renugopalakrishnan, R. Jose and S. Ramakrishna, *Mater. Sci. Eng. R*, 2009**, 63,** 81-99.

15 J. K. Lee and M. Yang, *Mater. Sci. Eng. B*, 2011, **176**, 1142-1160.

16 F. Yan, L. Huang, J. Zheng, J. Huang, Z. Lin, F. Huang and M. Wei, *Langmuir*, 2010, **26**, 7153-7156.

17 R. Scholin, M. Quintana, E. M. J. Johansson, M. Hahlin, T. Marinado, A. Hagfeldt and H. Rensmo, *J. Phys. Chem. C*, 2011, **115**, 19274-19279.

18 T. P. Chou, Q. Zhang and G. Cao, *J. Phys. Chem. C*, 2007**, 111**, 18804-18811.

19 H. Horiuchi, R. Katoh, K. Hara, M. Yanagida, S. Murata, H. Arakawa and M. Tachiya, *J. Phys. Chem. B*, 2003**, 107**, 2570-2574.

20 P. P. Das, S. A. Agarkar, S. Mukhopadhyay, U. Manju, S. B. Ogale and P. S. Devi, *Inorg. Chem*., 2014, **53**, 3961-3972.

21 S. Mukopadhyay, P. P. Das, S. Maity, P. Ghosh and P. S. Devi, *Applied Catalysis B: Environmental*, 2015, **165**, 128-138.

22 S. Mihaiu, I. Atkinson, O. Mocioiu, A. Toader, E. Tenea and M. Zaharescu, *Rev. Roum. Chim*., 2011, **56**, 465-472.

23 M. Batzill and U. Diebold, *Prog. Surf. Sci*., 2005, **79**, 47-154.

24 P. P. Das and P. S. Devi, *Inorg. Chem*., 2014, **53**, 10797-10799.

25 A. Jana, P. P. Das, S. A. Agarkar and P. S. Devi, *Solar Energy*, 2014, **102**, 143-151.

26 S. B. Ambade, R. S. Mane, A. V. Ghule, M. G. Takwale, A. Abhyankar, B. W. Chod, and S. H. Han, *Scripta Materialia*, 2009, **61**, 12-15.